

## Highly confined energy propagation in a gap waveguide composed of two coupled nanorod chains

F. M. Wang, H. Liu, T. Li, S. M. Wang, and S. N. Zhu<sup>a)</sup>

National Laboratory of Solid State Microstructures, Department of Physics, Nanjing University, Nanjing 210093, People's Republic of China

Jie Zhu and Wenwu Cao

Material Research Institute, The Pennsylvania State University, Pennsylvania 16802, USA

(Received 24 July 2007; accepted 8 September 2007; published online 26 September 2007)

We propose a subwavelength waveguide composed of two parallel nanorod chains. Based on the finite-difference time-domain analysis, we find that the electromagnetic energy can be highly confined in the gaps of nanorod pairs and transported in the gap waveguide through strong magnetic coupling interaction between neighboring nanorod pairs. In a structure with the rod length of 500 nm and the gap size of 100 nm, the energy flow cross section of the propagation mode can be restricted to the size of  $\lambda/33 \times \lambda/16$  at the frequency of 130.0 THz. The corresponding attenuation length of energy propagation reaches  $7.2\lambda$ . Moreover, these propagation modes exhibit a broad continuous frequency band from zero up to a cutoff frequency  $\omega_c \sim 162.6$  THz. © 2007 American Institute of Physics. [DOI: 10.1063/1.2790786]

Recently, chains of metal nanoparticles have been proposed for transport electromagnetic (EM) energy below the diffraction limit at visible and near-infrared frequencies.<sup>1-4</sup> Owing to the strong coupling between light and nanoparticles, the EM energy can be converted into oscillatory electron motions in nanoparticles. In one-dimensional metal nanoparticle chains resonant excitation results in the transporting of EM energy along the chains, but there is a high heating loss due to tight confinement of the mode to subwavelength scale. Although the two-dimensional metal nanoparticle square lattice with a lateral grading in nanoparticle size shows reduced heating loss, EM energy is localized in one dimension within a subwavelength region.<sup>4,5</sup> In the nanoparticle chain waveguide, the EM energy would be transported in a relatively narrow frequency band surrounding the resonance frequency. However, it has been reported that in a magnetic resonator chain,<sup>6</sup> energy transportation can be realized in a broad frequency range from zero up to a cutoff frequency  $\omega_c$ .

Recently, a lot of attention has also been focused on the plasmon of metal rods or wires in nanoscale for their potential applications.<sup>7-19</sup> It is well known that in a metal nanoparticle chain, light strongly couples with particles and the absorption cross section can be far exceeding the nanoparticle size, which leads to energy transportation along the chain, like a waveguide. If the nanoparticle is extended into a nanorod and two metal nanorods are aligned along a common axis with a small gap in between, the field can be drastically enhanced in the gap because of localized charges at the ends of the rods induced by the strong coupling.<sup>15</sup> When pairs of coupled nanorods are closely arrayed in the direction perpendicular to the nanorod axis, these gaps form a linear gap chain, as shown in Fig. 1. The chain is actually a subwavelength waveguide along which EM energy can be transported with low loss. In addition, it is noticed that this waveguide has a wide frequency band from zero up to a cutoff frequency. An attenuation length of about  $7.2\lambda$  can be

achieved in the configuration with the light confined to lateral and transverse dimensions of about  $\lambda/33$  and  $\lambda/16$ .

The waveguide system shown in Fig. 1 is in a vacuum environment. The dimensions of each metal rod are  $50 \times 50 \times 500$  nm<sup>3</sup>. The gap between the ends of the rod chains, i.e., the width ( $w$ ) of the gap, is 100 nm. The interval between two parallel adjacent rods ( $i$ ) is 150 nm. As mentioned above, the charges congregate at the rod ends under the excitation of light, which couples the light energy into the gap waveguide. As a consequence, the energy can be transported through the gap waveguide along the arrow in the  $x$  direction. Because the cross section of the energy flow confined between rod ends of each pair is relatively small (with high energy density and small mode size), the interval must be sufficiently small so that the neighboring rod pairs in the  $x$  direction can couple to each other and the energy can be transported along the gap waveguide. Increasing the size of the intervals will decrease the coupling strength as well as the energy flow. If the interval is large enough, for example, 800 nm, each pair of rod will resonate separately with very

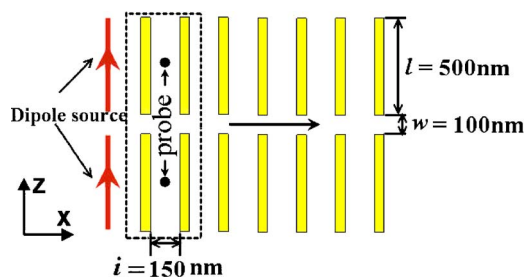


FIG. 1. (Color online) Schematic illustration of the gap waveguide composed of two coupling nanorod chains with the rod length  $l=500$  nm, waveguide width  $w=100$  nm, and the interval of two adjacent rods  $i=150$  nm. The dimensions of each rod are  $50 \times 50 \times 500$  nm<sup>3</sup>. The arrow in the waveguide shows the propagation direction of the energy in the gap waveguide. The red arrows in the left side represent two identical dipole sources, which are employed to excite the resonance in the waveguide. The two black point indicates the probes used to detect the local  $H$  field between the first two rod pairs.

<sup>a)</sup>Electronic mail: zhunsn@nju.edu.cn

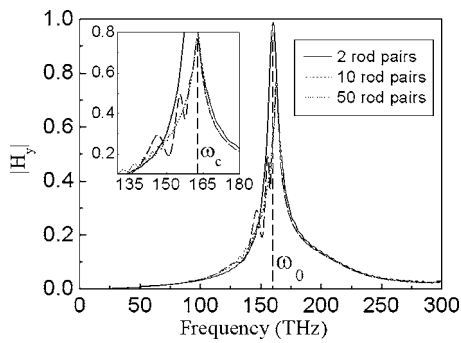


FIG. 2. Detected local  $y$  component of the  $H$  field vs frequency at a point between the first two rod pairs in 2 rod pair (black curve), 10 rod pair (dashed curve), and 50 rod pair (dotted curve) waveguide systems. The inset is the magnified figure in order to see more clearly the split resonance modes.  $\omega_0$  and  $\omega_c$  represent the eigenfrequency and cutoff frequency of the waveguide, respectively.

weak coupling between adjacent rod pairs; little energy can be propagated in this structure.

In our simulations, the system is excited by two identical dipole sources shown with two red arrows along the  $z$  axis (see Fig. 1), which are placed at a distance of 200 nm from the first rod pair in the  $x$  direction. The length of dipoles is equivalent to that of the nanorods. As each rod can be approximated as a dipole, the dipole sources are equivalent to a special pair of rods. In this case, the coupling between the sources and the first rod pair is similar to that between any nearby pairs of rods in the waveguide. Therefore, the EM energy can be easily coupled into and transported in the structure.

To study the EM energy transportation in a gap waveguide by the resonance of the nanorods, we perform a set of finite-difference time-domain (FDTD) calculations using a commercial software package CST MICROWAVE STUDIO (Computer Simulation Technology GmbH, Darmstadt, Germany). In the calculations, we rely on the Drude model to characterize the bulk metal properties. Namely, the metal permittivity in the infrared spectral range is given by  $\epsilon = 1 - \omega_p^2 / (\omega^2 + i\omega\gamma)$ , where  $\omega_p$  is the bulk plasma frequency and  $\gamma$  is the relaxation rate. For gold,<sup>20</sup> the characteristic frequencies fitted to experimental data are  $\omega_p = 1.37 \times 10^{16} \text{ s}^{-1}$  and  $\gamma = 4.08 \times 10^{13} \text{ s}^{-1}$ .

In the simulations, we employed a probe to detect the magnitude of magnetic ( $H$ ) field between rods in systems with 2 rod pairs, 10 rod pairs, and 50 rod pairs arrayed in the  $x$  direction. The probe is always placed between the first two rod pairs in the three cases. The magnitude of local magnetic field  $|H_y|$  vs frequency is shown in Fig. 2, from which we can determine the resonance modes of the gap waveguide. Firstly, we investigated the electromagnetic response of a two-rod pair structure, as shown in the dashed rectangular frame in Fig. 1. The amplitude  $|H_y|$  is greatly enhanced at 160.0 THz (black curve in Fig. 2), indicating that strong magnetic resonance has taken place at this frequency. In the rod array, each pair of neighboring rods, which forms an equivalent LC circuit, can be regarded as a magnetic resonator. As has been reported in Ref. 6, magnetic resonance mode will split into two nondegenerate modes in two closely placed magnetic resonators. Herein, in the multirod waveguide, due to strong coupling among these rod-pair resonators, the eigenmode splits into more resonance modes. These modes correspond to the burrs of  $|H_y|$  spectra in Fig. 2.

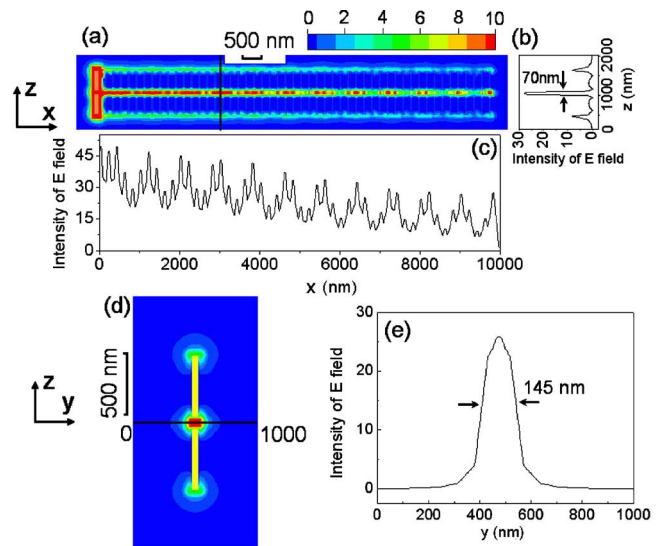


FIG. 3. (Color online) (a) The intensity of  $E$  field in the waveguide in the  $x$ - $z$  plane at a frequency of 130.0 THz. (b) and (c) show distribution of  $E$  field intensity along lines at  $x=3000$  nm and waveguide axis, respectively. (d) The intensity of  $E$  field in the cross section of the waveguide in the  $y$ - $z$  plane at a distance of 3000 nm from the left side of the waveguide. (e) The intensity of  $E$  field along the horizontal black line in Fig. 3(d).

dashed and dotted curves represent the detected local magnetic field between the first two rod pairs in systems with 10 and 50 rod pairs in the  $x$  direction, respectively. Obviously, as the rod number increases in the system, more resonance modes will appear, which are shown as burrs on the left side of the spectra peak. Note that all split resonance modes appear below a cutoff frequency (about 162.6 THz)  $\omega_c$  which is slightly higher than the eigenfrequency of 160.0 THz. If an infinite number of rods are placed along the  $x$  direction, there would exist infinite resonance modes in a broad frequency band below the cutoff frequency, which indicates that the energy can be transported in the gap waveguide in the whole frequency band  $[0, \omega_c]$ . Above the cutoff frequency, there is no resonance mode although the magnetic field is enhanced. In other words, no energy can propagate in the gap waveguide when  $\omega > \omega_c$ .

To investigate how the energy is transported in this waveguide, we utilized two identical dipole sources placed at a distance of 200 nm from the left side of the waveguide to excite the resonance modes. The simulated model structure contains 50 rod pairs along the  $x$  direction with a 100 nm gap in between the two chains. We assign open boundary conditions in the three dimensions,  $x$ ,  $y$ , and  $z$ , which mimic the actual environment in real experiments. The background of the waveguide is vacuum. If the nanorods are deposited on a dielectric substrate, the eigenfrequency and cutoff frequency would have slight redshift.

Figure 3(a) shows the intensity distribution of the electric ( $E$ ) field of the waveguide at the frequency of 130.0 THz which is lower than the cutoff frequency. As expected, the main part of the input power of the dipole source is coupled into the gap waveguide; only a small part of energy flows along the other ends of the rod arrays. In the  $z$  direction, the energy is confined to the gaps between the rod ends, which can be transported below the diffraction limit with low loss. In order to see the confinement of the energy in the  $z$  direction more clearly, we calculated the distribution of the  $E$  field intensity along a straight line at a distance of  $x=3 \mu\text{m}$  from

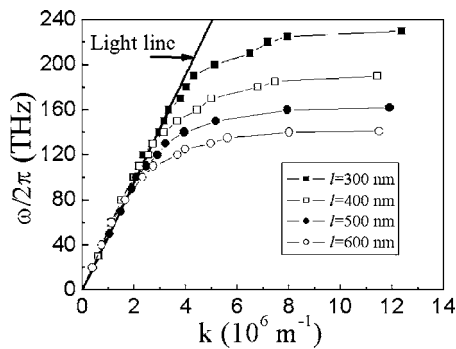


FIG. 4. Simulated dispersion relation of the waveguide with the rod length  $l$  equals 300 nm (curve with closed squares), 400 nm (curve with open squares), 500 nm (curve with closed circles), and 600 nm (curve with open circles), respectively. The black line is the dispersion relation of light in vacuum.

the front of the waveguide, as shown in Fig. 3(b). The energy is confined in a scale of 70 nm in the  $z$  direction. Compared to the single nanorod chain case, the field between the rod ends in the two coupled nanorod chains is greatly enhanced.<sup>15</sup> The structure also allows the enhancement of nonlinear light interactions for nonlinear host materials.

The attenuation length can be calculated from the intensity distribution of the  $E$  field along the gap waveguide axis in the  $x$  direction. At the frequency of 130.0 THz, the attenuation length is about  $16.6 \mu\text{m}$  ( $7.2\lambda$ ). The absolute value of attenuation length is comparable to that ( $15.4 \mu\text{m}$ ,  $3.7\lambda$ ) reported in Ref. 6 at 73 THz. However, in the waveguide proposed in this paper the energy transportation can be realized at a much higher frequency and in a much smaller scale below the diffraction limit.

Besides the confinement of the energy in the  $z$  direction, the structure can also highly restrict the energy in the  $y$  direction. As a result, the energy is confined in two dimensions of the gap waveguide. Figure 3(d) shows the intensity distribution of the  $E$  field in the waveguide in the  $y$ - $z$  cross section. Along the black straight line in Fig. 3(d), the intensity distribution of  $E$  field along the  $y$  direction is presented in Fig. 3(e). From the intensity of  $E$  field in Figs. 3(b) and 3(e), the transverse mode size of the waveguide can be determined to be  $70 \times 145 \text{ nm}^2$  ( $\lambda/33 \times \lambda/16$ ). Note that the transverse mode size is directly related to the gap size between rod ends. If the two rod chains are arrayed closer, for example, 50 nm, the transverse mode size can reach 40 nm. However, most of the energy will be squeezed into the rod ends if the gap between rod ends is extremely small, say around 10 nm, which would produce very large loss.

The cutoff frequency of the waveguide increases with decreasing rod length  $l$ . Figure 4 shows the dispersion relation calculated by FDTD simulation method for EM waves propagating in a waveguide system with 50 rod pairs in the  $x$  direction. The Drude model is employed to fit the characteristics of the gold. In our simulation, the  $E$  field distribution in the waveguide is analyzed to determine the wavevector of the propagation mode. With increasing wave vector  $k$ , the frequency approaches a constant and the slope of the curve decreases, which indicates a decrease of the group velocity of the EM wave. This dispersion relation closely resembles the behavior of surface plasmon polaritons (SPPs) and spoof SPPs (Ref. 21) propagating along metal wires and corrugated

metal wires at optical and terahertz frequencies, respectively. The upper limit of the frequency band can be tuned by changing the rod length. For a gap of 100 nm between rod ends, the cutoff frequency will increase from 140 to 235 THz when the rod length decreases from 600 to 300 nm. Based on the experimental data<sup>20</sup> of the metal parameters in the frequency range where the Drude model cannot be applied, energy transportation in this gap waveguide can even be realized at visible frequencies when the rod length is reduced to 100 nm.

In conclusion, we have proposed a type of subwavelength gap waveguide that can be used to transport energy below the diffraction limit in a broad frequency band. The energy can be highly confined in subwavelength regions of  $\lambda/33$  and  $\lambda/16$  in the propagation cross section at the frequency of 130.0 THz. This configuration can be easily tuned to realize energy transportation at a much higher frequency range by decreasing the size of the rods. This simple structure has the capability to produce very high intensity  $E$  field in the gap waveguide, which has potential applications in biosensing and in-plane transmission of EM energy for subwavelength integrated optical devices.

This work is supported by the State Key Program for Basic Research of China (Nos. 2006CB921804 and 2004CB619003) and the National Natural Science Foundation of China under Contract Nos. 10534042, 60578034, 10604029, and 10704036.

- <sup>1</sup>M. Quinten, A. Leitner, J. R. Krenn, and F. R. Aussenegg, *Opt. Lett.* **23**, 1331 (1998).
- <sup>2</sup>J. R. Krenn, A. Dereux, J. C. Weeber, E. Bourillot, Y. Lacroute, J. P. Gouyonnet, G. Schider, W. Gotschy, A. Leitner, F. R. Aussenegg, and C. Girard, *Phys. Rev. Lett.* **82**, 2590 (1999).
- <sup>3</sup>M. L. Brongersma, J. W. Hartman, and H. A. Atwater, *Phys. Rev. B* **62**, R16356 (2000).
- <sup>4</sup>S. A. Maier, M. D. Friedman, P. E. Barclay, and O. Painter, *Appl. Phys. Lett.* **86**, 071103 (2005).
- <sup>5</sup>E. Ozbay, *Science* **311**, 189 (2006).
- <sup>6</sup>H. Liu, D. A. Genov, D. M. Wu, Y. M. Liu, J. M. Steele, C. Sun, S. N. Zhu, and X. Zhang, *Phys. Rev. Lett.* **97**, 243902 (2006).
- <sup>7</sup>C. Sönnichsen, T. Franzl, T. Wilk, G. von Plessen, J. Feldmann, O. Wilson, and P. Mulvaney, *Phys. Rev. Lett.* **88**, 077402 (2002).
- <sup>8</sup>J. C. Weeber, A. Dereux, C. Girard, J. R. Krenn, and J. P. Gouyonnet, *Phys. Rev. B* **60**, 9061 (1999).
- <sup>9</sup>F. Neubrech, T. Kolb, R. Lovrincac, G. Fahsold, A. Pucci, J. Aizpurua, T. W. Cornelius, M. E. Toimil-Molares, R. Neumann, and S. Karim, *Appl. Phys. Lett.* **89**, 253104 (2006).
- <sup>10</sup>T. Laroche and C. Girard, *Appl. Phys. Lett.* **89**, 233119 (2006).
- <sup>11</sup>H. Ditlbacher, A. Hohenau, D. Wagner, U. Kreibitz, M. Rogers, F. Hofer, F. R. Aussenegg, and J. R. Krenn, *Phys. Rev. Lett.* **95**, 257403 (2005).
- <sup>12</sup>S. K. Gray and T. Kupka, *Phys. Rev. B* **68**, 045415 (2003).
- <sup>13</sup>R. M. Dickson and L. A. Lyon, *J. Phys. Chem. B* **104**, 6095 (2000).
- <sup>14</sup>K. Imura, T. Nagahara, and H. Okamoto, *J. Chem. Phys.* **122**, 154701 (2005).
- <sup>15</sup>J. Aizpurua, G. W. Bryant, L. J. Richter, F. J. García de Abajo, B. K. Kelley, and T. Mallouk, *Phys. Rev. B* **71**, 235420 (2005).
- <sup>16</sup>J. R. Krenn, B. Lamprecht, H. Ditlbacher, G. Schider, M. Salerno, A. Leitner, and F. R. Aussenegg, *Europhys. Lett.* **60**, 663 (2002).
- <sup>17</sup>S. A. Maier, P. G. Kik, and H. A. Atwater, *Appl. Phys. Lett.* **81**, 1714 (2002).
- <sup>18</sup>F. M. Wang, H. Liu, T. Li, Z. G. Dong, S. N. Zhu, and X. Zhang, *Phys. Rev. E* **75**, 016604 (2007).
- <sup>19</sup>H. S. Chu, W. B. Ewe, E. P. Li, and R. Vahldieck, *Opt. Express* **15**, 4216 (2007).
- <sup>20</sup>P. B. Johnson and R. W. Christy, *Phys. Rev. B* **6**, 4370 (1972).
- <sup>21</sup>S. A. Maier, S. R. Andrews, L. Martín-Moreno, and F. J. García-Vidal, *Phys. Rev. Lett.* **97**, 176805 (2006).